Supporting Information

Unlocking the Potential of Amorphous Red Phosphorus Films as Long-term Stable Negative Electrode for the Lithium Battery

Chandrasekar M Subramaniyam[#,§], Zhixin Tai[#], Nasir Mahmood[#], Dan Zhang[#], Hua Kun Liu[#,*], John B Goodenough[§], Shi Xue Dou[#]

[#] Institute for Superconducting and Electronic Materials, Australian Institute of Innovative Materials, Innovation Campus, University of Wollongong, North Wollongong, NSW 2500 Australia

[§] Texas Materials Institute, Department of Mechanical Engineering, 204 E. Dean Keeton Street, C2200, University of Texas Austin, Texas 78712 USA

*corresponding author's Email ID: hua@uow.edu.au

Experimental details

All chemicals used were of laboratory grade, purchased from Sigma Aldrich, and used without any further treatment.

Preparation of nanostructured red phosphorus (NS-RP)

NS-RP was prepared from commercial RP by high-energy ultrasonication with an ultrasonic processors (Model: VC505-VC750, Sonics & Materials INC, USA). In a typical synthesis, 1 g of red phosphorus was dispersed in 20 ml distilled water. This solution was then subjected to high-energy sonication for 20 h in an ice-cooled water bath at an amplitude of 35 with 2 s pulse time for each on and off pulse. The temperature of the solution was maintained at < 25 °C by the constant addition of ice cubes into the surrounding water bath. The as-obtained solution was then frozen in a liquid-nitrogen bath and subjected to freeze-drying at -55 °C for 3 days. The product was labelled as NS-RP for further analysis.

Preparation of NS-RP-rGO hybrid

Three different RP − reduced-graphene-oxide (rGO) hybrids containing 10, 20, and 30 wt.% rGO were prepared. Appropriate quantities of NS-RP and rGO were put into 20 ml DD H_2O and subjected to ultrasonication for 3 h at an amplitude of 35 with 2 s pulse time for each on and off pulse. The obtained precursor was freeze-dried at -55 °C for 3 days and labelled as NS-RP@rGO-10, NS-RP@rGO-20, and NS-RP@rGO-30, respectively.

Material characterizations

All samples were subjected to physical and electrochemical characterizations. Phase purities were determined by X ray diffraction (XRD; GBC MMA) with Cu K_α irradiation at 1°/min scan rate and 0.02° step size. Morphologies and their compositions were analysed by field-emission-gun-scanning electron microscopy (FEGSEM, JOEL) operated at 5 V and 10 μA, while particle sizes and particle size distributions were determined by transmission electron microscopy (TEM, JOEL JEM 2010) operated at 200 kV with a resolution of 10 Å and processed with Gatan Micrograph software and nanosheet's depth profile was determined using atomic forced microscopy (AFM, Asylum Research MFP-3D Scanning probe microscopy, SPM). The structures and compositions were also analysed by Raman spectroscopy. X ray photoelectron spectroscopy (XPS) was used to determine the surface composition and the valence states of the respective elements. Nitrogen adsorption-desorption studies were performed with a Quantachrome (iQ-MP) for Brunauer-Emmett-Teller (BET) surface-area analysis.

Electrochemical Characterization

All samples were tested in a classical CR 2032 coin cell in a two-electrode system against $Li^+/Li°$. A slurry containing an 8:1:1 wt. ratio of active material (NS-RP) to carbon Super P (as conducting agent) to polyvinylidene fluoride (PVDF as binder) was prepared with N-methyl-2-pyrrolidone (NMP), as blending solvent in a planetary mixer. Electrodes were prepared from

the NS-RP@rGO hybrid composites in a weight ratio of 7:1.5:1.5 with carboxymethyl cellulose (CMC) as binder and Super P carbon with DD water as solvent. The obtained slurry was tape cast over copper foil with a doctor blade 50 μm in thickness and vacuum dried at 120 °C (for PVDF binder) and 80 °C (for CMC binder) overnight. The electrodes were cut into disks, and each disk was loaded with 1 $mg.cm^{-2}$ active materials, ~0.5 mg of active materials. The cells were fabricated in an argon-filled glove box maintained at less than 0.1 ppm O_2 and H_2O and tested as anodes for LIBs. The NS-RP hybrid electrode was used as the working electrode with Li foil as reference/counter electrode separated by Celgard, soaked in a few drops of 1 M $LiPF_6$ (in 1:1 v/v ethylene carbonate/ diethyl carbonate (EC/DEC)) as electrolyte. All cells were rested overnight to reach equilibrium and exhibited an open circuit voltage of 2.9-3.0 V against Li^+/Li^0. The cells were tested galvanostatically in an advanced multichannel battery tester (Land CT2001A, China) between 0.002 and 3 V against Li^+/Li^0. The galvanostatic intermittent titration technique (GITT) measurements consisted of a series of current pulses applied to the coin cells at a low current density of 100 mAg^{-1} for 20 minutes, each followed by a 90 minute recess to allow full relaxation of lithium diffusion, so as to reach equilibrium potential and to minimize the self-discharge of RP during the test. Cyclic voltammetry (CV) and electrochemical impedance spectroscopy (EIS) were conducted with Biologic VMP3 instruments. CV was conducted with scanning at 0.1 mVs^{-1} between 0.002 and 3.00 V, while EIS was conducted by applying a sine wave 5 mV in amplitude over the frequency range of 0.1 MHz to 10 mHz.

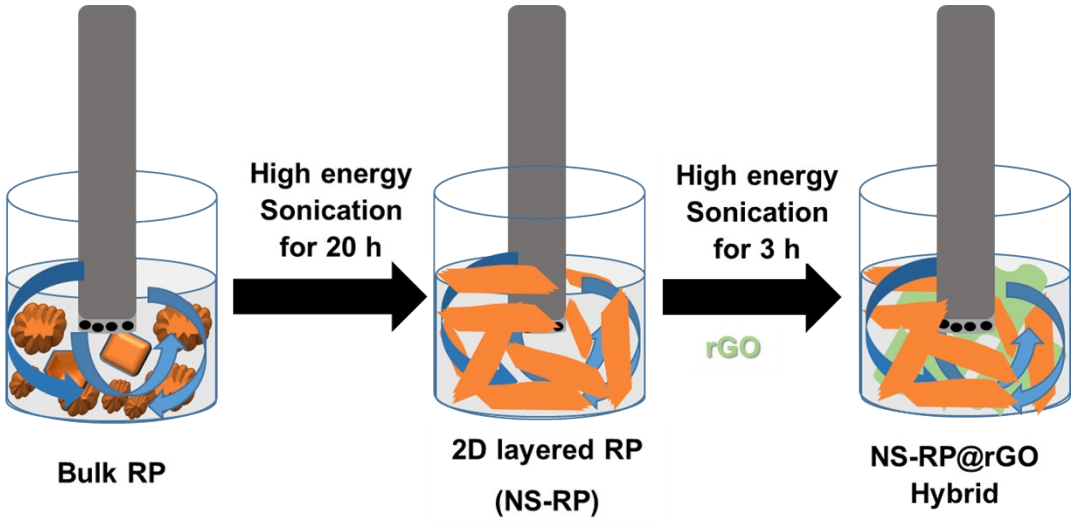

Scheme 1 Schematic illustration of the synthesis of amorphorus RP films (NS-RP) from bulk RP and synthesis of its hybrid with rGO (NS-RP@rGO).

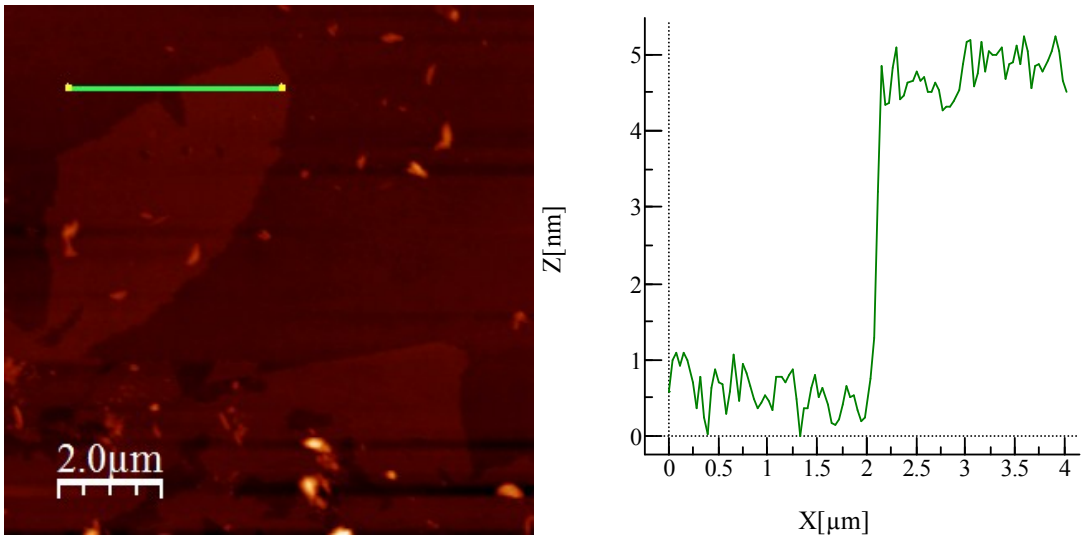

Fig. S0 AFM topography image and depth profile of the NS-RP. The topography show nanosheet morphology of the NS-RP whose thickness is ~4.8 nm.

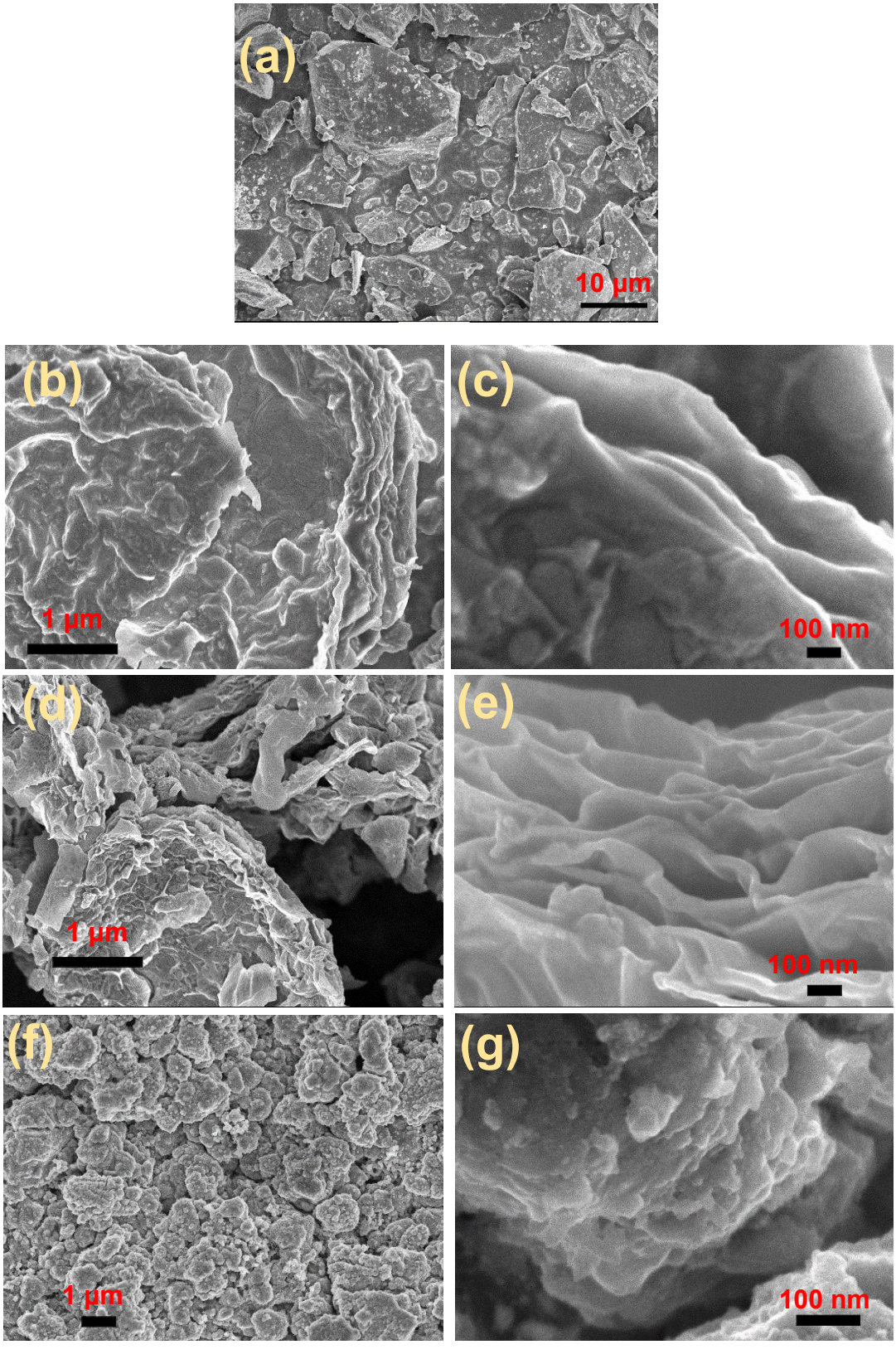

Fig. S1 FESEM images showing the morphology of (a) bulk RP; (b-c) NS-RP@rGO-10; (d-e) NS-RP@rGO-20; (f-g) NS-RP after 100 cycles

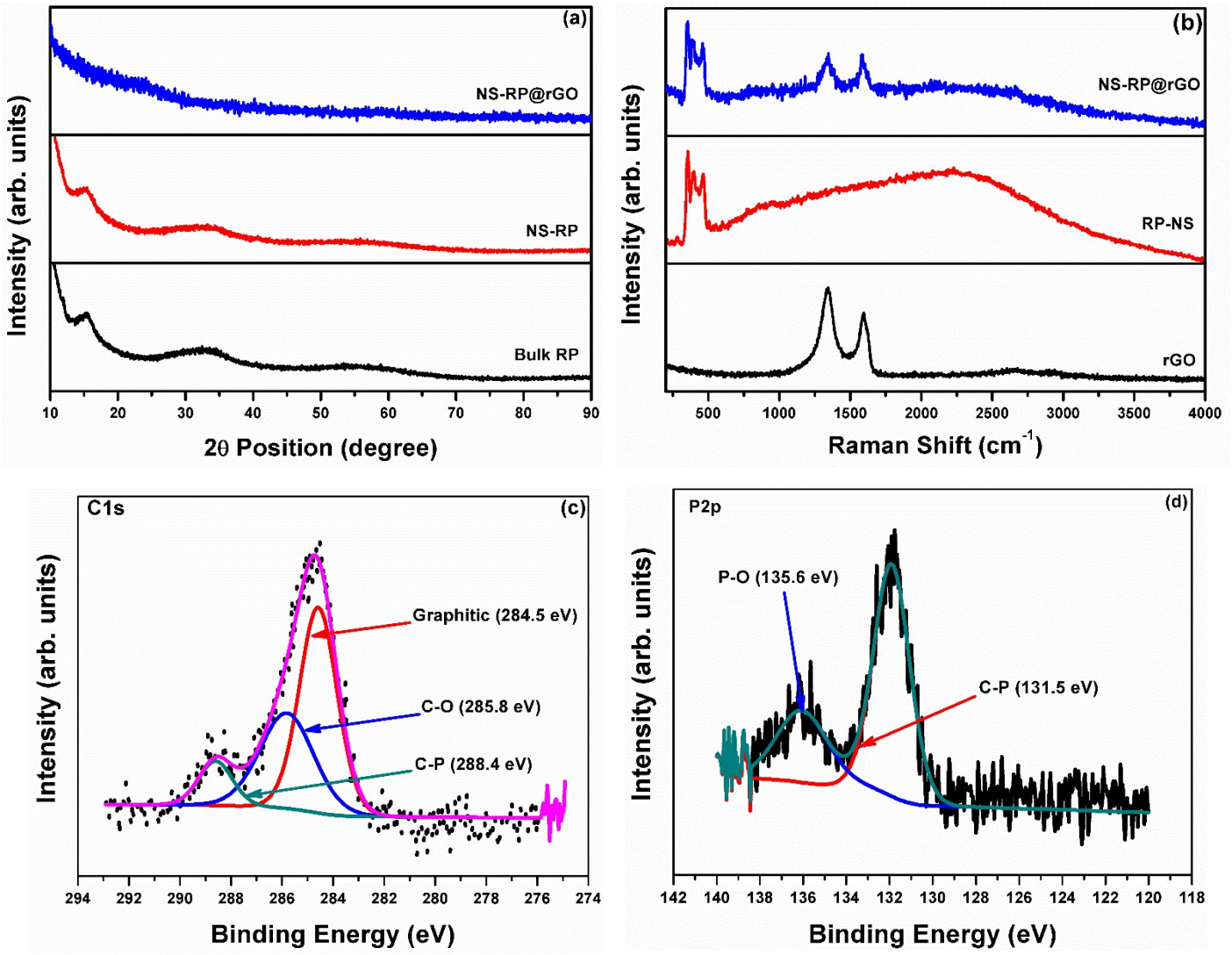

Fig. S2 (a) X ray diffraction patterns and (b) Raman spectra of bulk and amorphous films of red phosphorus (RP) and NS-RP@rGO hybrid composite; high resolution XPS spectra of the (c) C 1s and (d) P 2p regions for the NS-RP@rGO hybrid.

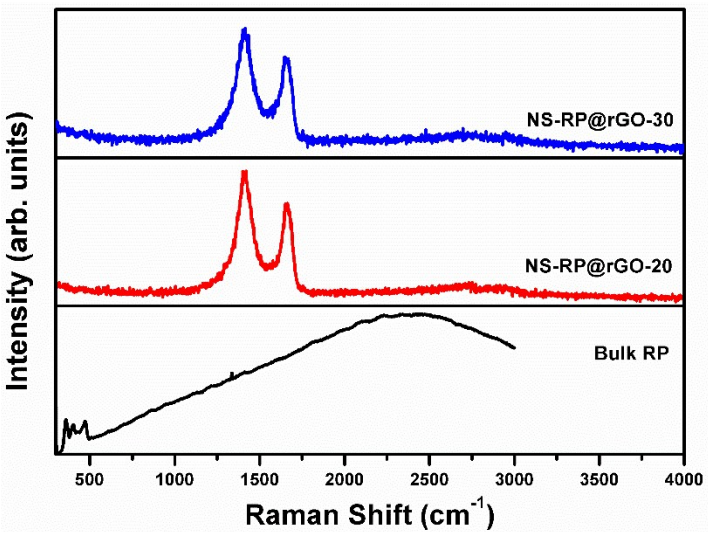

Fig.S3 Raman spectra of bulk RP; NS-RP@rGO-20; and NS-RP@rGO-30 hybrid composites.

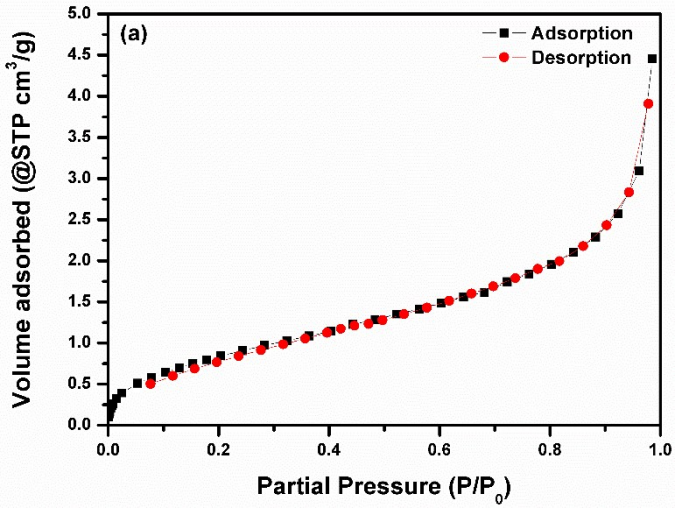
(a)
Adsorption
Desorption
Volume adsorbed (@STP cm3/g)
Partial Pressure (P/P0)
0.0
0.5
1.0
1.5
2.0
2.5
3.0
3.5
4.0
4.5
5.0
0.0
0.2
0.4
0.6
0.8
1.0

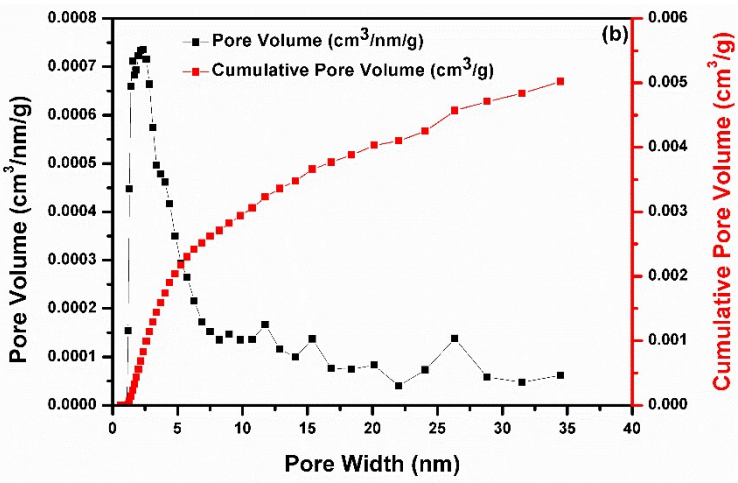
(b)
Pore Volume (cm3/nm/g)
Cumulative Pore Volume (cm3/g)
Pore Volume (cm3/nm/g)
Cumulative Pore Volume (cm3/g)
Pore Width (nm)
0.0000
0.0001
0.0002
0.0003
0.0004
0.0005
0.0006
0.0007
0.0008
0.000
0.001
0.002
0.003
0.004
0.005
0.006
0
5
10
15
20
25
30
35
40

Fig. S4 (a) N_2 adsorption-desorption isotherms and Barrett-Joyner-Halenda (BJH) pore size distributions amorphous RP films.

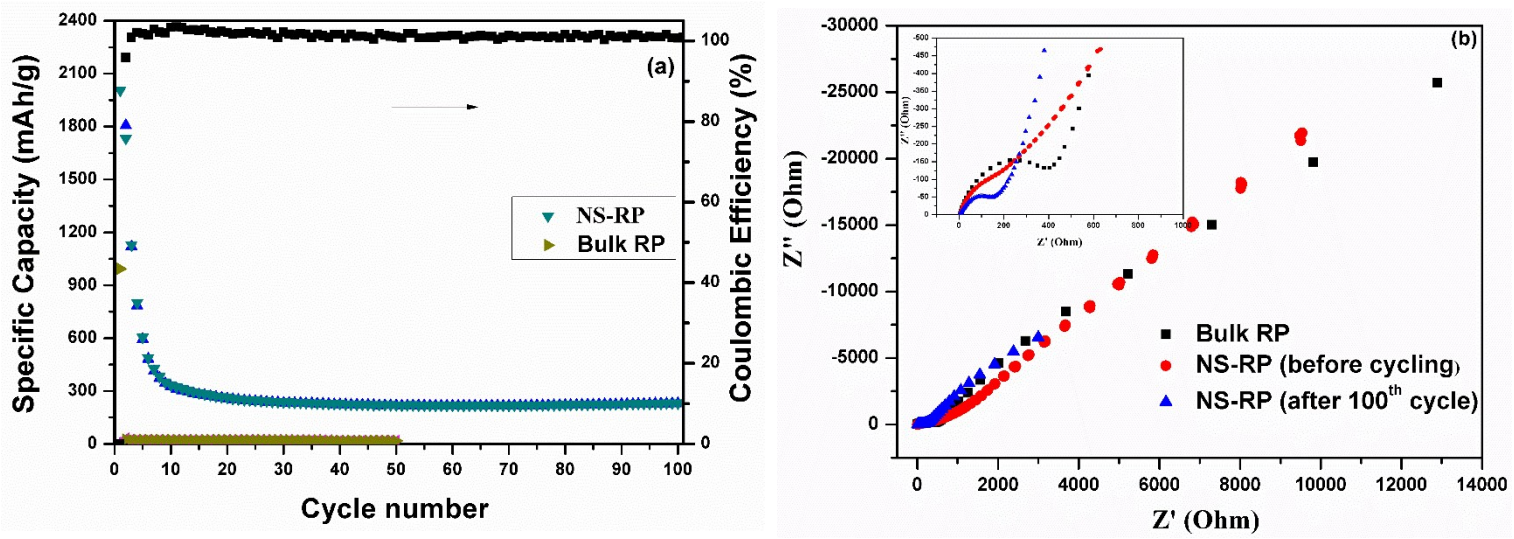

Fig. S5 (a) Long-term cycling stability at 100 mAg^{-1} compared with bulk RP; (b) Electrochemical impedance spectra of samples (inset: enlargement at high frequency)

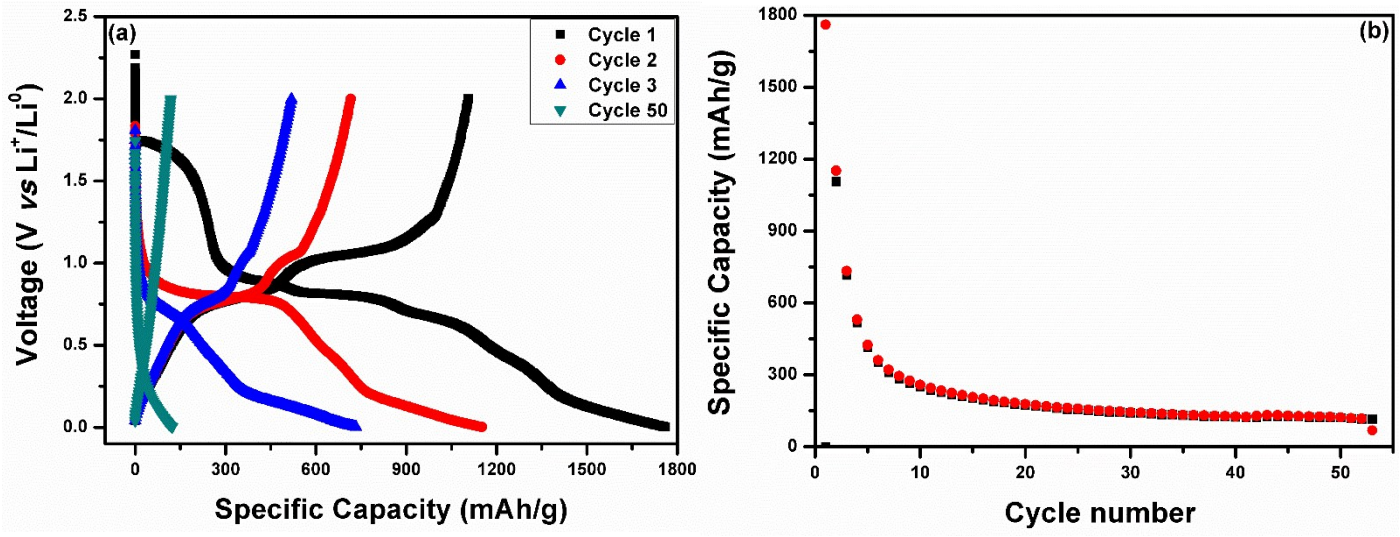

Fig. S6 Electrochemical performance of NS-RP *vs.* Li^+/Li^0 at 50 mAg^{-1} between 0.002 - 2 V: (a) voltage profiles for selected cycles and (b) cycling performance.

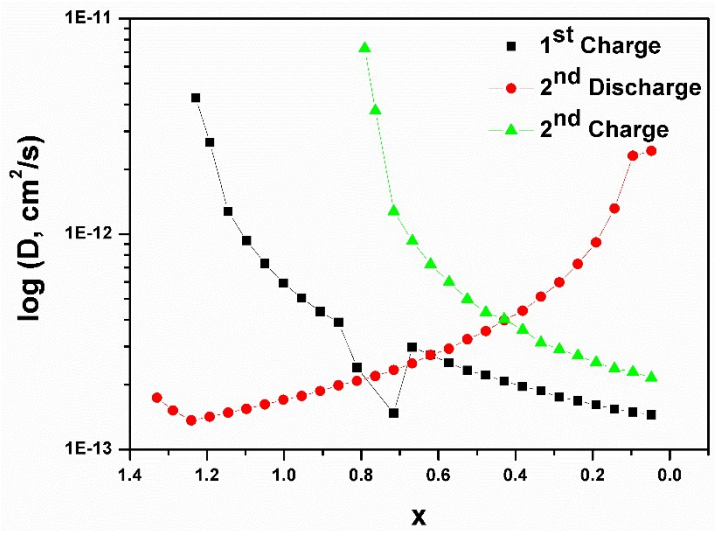

Fig. S7 Li^+ chemical diffusion coefficient of NS-RP determined by GITT during the charge-discharge process

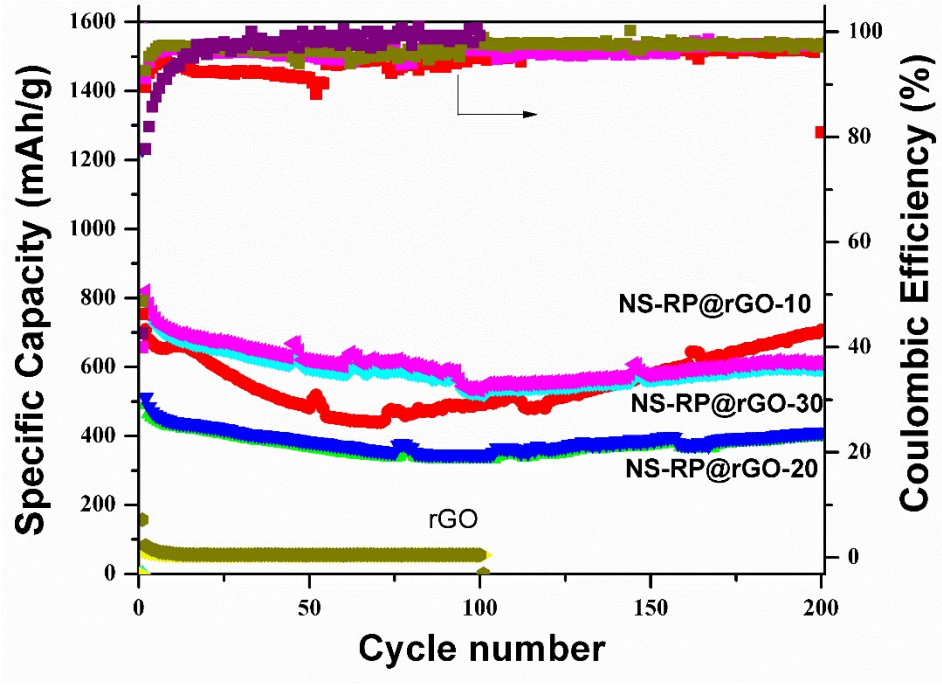

Fig. S8 Long-term cycling performance of NS-RP@rGO composites at 50 mAg^{-1}.